Chapter 6 Interactions of π-conjugated Organic Molecules with the Si(100) Surfaces

6.1 Motivation

For π-conjugated molecules to be used as conductors or semiconductors, they must retain π-conjugation, even after adsorption. Benzene, a simple π-conjugated ring, is known to chemisorb on the Si(001) surface by forming Si-C bonds [1-3]. However, the formation of these new Si-C bonds results in the loss of π-conjugation and therefore is expected to dramatically decrease the electron transport capability of the molecule. This problem can be avoided by using specific functional groups that are not an intrinsic part of the delocalized π-system but which can tether the molecule of interest to the surface. For example, benzonitrile ($C_6H_5C{\equiv}N$) is known to selectively bond to the Si(100) surface through the external cyano substituent group [4]. Because the C≡N bond external to the ring exclusively interacts with the surface, the π-conjugation of the aromatic ring remains unperturbed upon chemisorption.

Benzaldehyde and acetophenone containing a conjugated phenyl ring and a carbonyl group may selectively bind to Si(100) through a typical 1,2-dipolar cycloaddition of the carbonyl group with a Si-dimer, leaving its phenyl ring skeleton intact on Si(100). This possibility was demonstrated in simple carbonyl containing compounds on Si(100) [5-12]. The other possibilities are that it can bind to the Si surface through its phenyl ring in similar binding modes to those of benzene [1-3] and its

derivatives [13-14]. Thus, for benzaldehyde and acetophenone containing a conjugated carbonyl and phenyl ring, rich attachment chemistry on Si(100)can be expected.

6.2 Benzaldehyde adsorption

6.2.1 High-resolution electron energy loss spectroscopy

Figure 6.1 shows the high-resolution electron energy loss spectra of the physisorbed and the saturated chemisorbed benzaldehyde on Si(100)-2×1. These spectra were obtained using an on-axis Si(100) sample that was cooled to 110 K. The vibrational frequencies and their assignments for physisorbed and chemisorbed benzaldehyde on Si(100)-2×1 are listed in Table 6.1. This table shows that the vibrational features of physisorbed benzaldehyde (Figure 6.1a) are in excellent agreement with the IR spectrum of liquid benzaldehyde [15]. Vibrational signatures at 470, 744, 853, 1027, 1193, 1431, 1598, 1713, 2791, and 3075 cm^{-1} can be clearly identified in the spectrum of physisorbed molecules. Among these vibrational signatures, the peak at 1713 cm^{-1} is assigned to the C=O stretching mode; the losses at 2791 and 3075 cm^{-1} are attributable to the $C(sp^2)$-H (-CHO) stretching mode and the $C(sp^2)$-H stretching mode on the phenyl ring, respectively. Additionally, vibrational features around 1598, 1431, and 1193 cm^{-1} are associated with the characteristic vibrational modes of the mono-substituted phenyl ring.

The vibrational features of chemisorbed benzaldehyde (Figure 6.1b) were obtained by annealing the multilayer benzaldehyde-covered sample to 300 K to drive away all the physisorbed molecules and leaving only a chemisorbed monolayer. Losses at 449, 521, 693, 789, 1019, 1191, 1430, 1604, 2884, and 3075 cm^{-1} can be readily resolved. The absence of the Si-H stretching around 2050 cm^{-1} [16] suggests the nature of molecular chemisorption for benzaldehyde on Si(100)-2×1. This result is consistent with the fact

that there is no observation of the Si-H stretching mode for acetaldehyde/Si(100) system around 300-400 K [6]. Compared to the physisorbed molecules, the vibrational peak around 1713 cm^{-1} associated with the C=O stretching mode is absent in the chemisorbed molecules. This demonstrates the rehybridization of carbon atoms of the C=O group and their involvement in binding with the Si surface. This is further supported by the appearance of the C (sp^3)-H (at 2884 cm^{-1}) stretching mode and the absence of the C(sp^2)-H (-CHO) stretching mode at 2791 cm^{-1} in the chemisorbed molecules [17]. A larger up-shift of around 90 cm^{-1} is observed for the C-H (-CHO) stretching due to the weaker inductive effect of the oxygen atom of chemisorbed benzaldehyde than that of the oxygen atom of physisorbed molecules. This assignment is further confirmed by another HREELS study of benzadehyde-α-d_1 as described in the following paragraph. Furthermore, the characteristic vibrational modes [ν(C-C)] of a monosubstituted phenyl ring around 1550-1650, 1400-1515, and 1150-1350 cm^{-1} [18-19] are retained in the HREELS spectra of chemisorbed benzaldehyde (Figure 6.1b), indicating the preservation of aromaticity of the phenyl ring.

In order to further confirm our assignments, benzadehyde-α-d_1 was also employed in our HREELS experiments. Parts a and b of Figure 6.2 present the vibrational features of physisorbed and saturated chemisorbed benzadehyde-α-d_1 on Si(100)-2×1, respectively. In Figure 6.2a, vibrational peaks at 454, 753, 859, 1001, 1191, 1457, 1599, 1703, 2104, and 3070 cm^{-1} are clearly resolved. Their assignments listed in table 6.1 show that the vibrational features of physisorbed molecules are in good accordance with the IR spectrum of liquid benzadehyde-α-d_1 [15]. Among there vibrational signatures, the two peaks at 1703 and 2104 cm^{-1} are assigned to C=O and C (sp^2)-D (-CDO) stretching

modes, respectively. The peak at 3070 cm^{-1} is ascribed to the C (sp^2)-H stretching of the phenyl ring. For chemisorbed molecules, the absence of observable intensity around 2900 cm^{-1} suggests that there are no carbon atoms on the phenyl ring rehybridizing from sp^2 into sp^3 after chemisorption. In addition, both C (sp^2)-D (-CDO) and C=O stretching modes are absent. Moreover, a new peak, attributable to the C^{sp3}-D stretching vibration, appears around 2184 cm^{-1}. A larger up-shift for the C-D (-CDO) stretching also shows that the oxygen atom directly interacts with the surface. Indeed, the fact that these changes occurred at the C-D and C-H stretching region upon chemisorption of benzadehyde-α-d_1 strongly supports the conclusion that only the C=O bond directly participates in the covalent binding with the surface.

6.2.2 X-ray photoelectron spectroscopy

Figure 6.3 presents the O 1s XPS spectra for physisorbed and chemisorbed benzaldehyde on Si(100)-2×1. O 1s photoemission spectrum of physisorbed molecules (Figure 6.3a) shows a symmetric peak at 533.3 eV with a typical FWHM (~1.2 eV) under our XPS resolution. The 533.3 eV binding energy observed here is close to the value observed for oxygen atoms in molecules containing intact carbonyl groups [5, 6, 9, 11]. Compared to the physisorbed spectrum, the O 1s (532.0 eV) core level of chemisorbed molecules (Figure 6.3b) displays a downshift of 1.3 eV, implying the direct involvement of the O-atom in benzaldehyde binding on Si(100)-2×1. This value is very close to that observed for phenanthrenequinone (532.4 eV) and for 1,2-cyclohexanedione (532.4eV) [9] chemisorbed on the Si(100) surface. Consequently, the O (1s) binding energy is consistent with the formation of a Si–O linkage for benzaldehyde binding on the Si(100) surface.

Figure 6.4 shows the fitted C 1s XPS spectra for physisorbed and chemisorbed benzaldehyde on Si(100)-2×1. The C 1s spectrum of physisorbed molecules is deconvoluted into two peaks centered at 288.2(14.5 %), and 285.5 (85.5 %) eV with an area ratio of 1:5.9 (Figure 6.4a). The peak at 288.2 eV can be assigned to the C atom of carbonyl, similar to the value obtained in molecules containing intact carbonyl groups [5, 6, 9, 11]. The photoemission feature at 285.5 eV is associated with the C atoms of phenyl ring [20].

For chemisorbed benzaldehyde ($C_6H_5C^{\alpha}HO$) (Figure 6.4b), the C 1s spectrum is significantly different, which implies large changes in electronic structures upon chemisorption. It can be fitted into two peaks at 286.3 (14.2 %) and 285.1 (85.8 %) eV with an area ratio of 1:6. These constituent C 1s peaks can be attributed to the C^{α} (286.3eV) atom and the C_6 (285.1 eV) atoms of the reaction adduct C_6H_5 (Si)C^{α} H-O(Si). Compared to the physisorbed molecules, the C 1s core level of the C=O group displays obvious down shift by 1.9 eV, which suggests that the C=O group is directly involved in the binding with the silicon surface. The rehybridization of the O and C^{α} atoms of the carbonyl groups and their bonding to silicon atoms with a much lower electronegativity (Pauling electronegativity =1.90) reduce the electronic polarization in the C^{α}-O. Thus, compared to the physisorbed benzadehyde, a much higher electron density is expected at the C^{α} atom, leading to a lower C 1s BE of the C^{α} atom. Besides, the C 1s core-level of the six C atoms in phenyl ring also displays a downshift of 0.4 eV upon chemisorption. In fact, the decrease in C 1s BE of a phenyl ring from 285.5 to 285.1 eV is attributable to the weaker inductive effect of the -(Si)C-O(Si)- group in chemisorbed benzaldehyde than that of the –C=O group in physisorbed molecule.

6. 2. 3 Scanning tunneling microscopy

In order to further elucidate the site-selectivity of benzaldehyde binding on Si(100)-2×1, STM was used to investigate the extent and spatial distribution of the present surface reaction system at atomic resolution. Figure 6.5a shows STM constant current topograghs (CCTs) of a clean Si(100)-2×1 surface at room temperature with a defect density of < 5 %. Figure 6.5b shows a room-temperature STM image obtained after a clean Si(001) surface was exposed to 0.01 L of benzaldehyde. At low coverage, individual molecules can be imaged in their preferred adsorption geometry without steric interaction from other molecules. A type of protrusion is visible, as depicted in Figure 6.5b. It appears to be on a dimer row, but is shifted slightly to one side of the row. While such small deviations can sometimes be caused by asymmetric STM tips, the slight sideway shift occurs randomly on each side of the dimer rows, suggesting that it is related to inherent asymmetry in the structure of the surface-bound molecules. Statistics counting performed on several images indicate that there is one preferred bonding state for benzaldehyde binding on Si(100), consistent with the vibrational results.

6.3 Acetophenone adsorption

6.3.1 High-resolution electron energy loss spectroscopy

Figure 6.6 shows the high resolution electron energy loss spectra of acetophenone-exposed Si(100)-2×1 at 110 K as a function of exposure. The vibrational frequencies and their assignments for physisorbed and chemisorbed molecules are summarized in Table 6.2. Vibrational signatures at 593, 738, 991, 1301, 1435, 1573, 1687, 2930, and 3055 cm^{-1} can be clearly identified in the spectrum of physisorbed molecules. Table 6.2 shows that the vibrational features of physisorbed acetophenone (Figure 6.6a) are in excellent

agreement with the IR spectrum of liquid acetophenone [21]. Among these vibrational signatures of physisorbed molecules, the peak at 2930 cm^{-1} is assigned to the C(sp^3)-H (-CH_3) stretching mode; the loss feature at 3055 cm^{-1} is attributable to the stretching mode of C(sp^2)-H on phenyl ring; the C=O stretching mode can account for the feature at 1687 cm^{-1}; vibrational features around 1573, 1435, and 1301 cm^{-1} are associated with the characteristic vibrational modes of monosubstituted phenyl ring.

The vibrational features of chemisorbed acetophenone (Figure 6.6b) obtained by annealing the multilayer acetophenone-exposed sample to 300 K to drive away all the physisorbed molecules are significantly different. Losses at 489, 681, 753, 1017, 1291, 1422, 1568, 2930, and 3055 cm^{-1} can be readily resolved. The absence of observable Si-H stretching around 2000–2100 cm^{-1} (Ref.16) suggests the nature of molecular chemisorption for acetophenone on Si(100)-2×1. Compared to physisorbed molecules, the vibrational peak around 1687 cm^{-1} associated to the C=O stretching mode is absent in chemisorbed molecules, demonstrating the rehybridization of carbon atoms of the C=O group and their involvement in binding with the Si surface. This is further supported by the appearance of two new peaks at 489 and 681 cm^{-1}, ascribed to Si-C and Si-O stretching modes [22, 23], respectively. On the other hand, the peak that appears around 2930 cm^{-1} may be attributed to the CH_3 stretching modes from the carbonyl methyl group or from the C (sp^3)-H stretching modes of phenyl ring due to rehybridization from sp^2 into sp^3 after chemisorption. To order to confirm this assignment, acetophenone-α-d_3 on Si(100)-2×1 was also employed in our HREELS experiments.

Figures 6.7a and 6.7b present the vibrational features of physisorbed and saturated chemisorption acetophenone-α-d_3 on Si(100)-2×1, respectively. In Figure 6.7a,

vibrational peaks at 581, 711, 886, 1024, 1267, 1445, 1582, 1695, 2275, and 3050 are clearly resolved. Their assignments listed in Table 6.2 show that the vibrational features of physisorbed molecules are in good accordance with the IR spectrum of liquid acetophenone-α-d_3 [21]. Among these vibrational signatures, the two peaks at 2275 and 1695 cm^{-1} are assigned to C(sp^3)-D (-CD_3) and C=O stretching modes, respectively. The feature at 3050 cm^{-1} is ascribed to the C (sp^2)-H stretching of phenyl ring. For chemisorbed molecules, the C=O stretching mode at 1695 cm^{-1} is absent. This demonstrates the rehybridization of carbon atoms of the C=O group and their involvement in binding with the silicon surface. In addition, the fact of no observable intensities around 2900 cm^{-1} suggests that there are no carbon atoms of phenyl ring rehybridizing from sp^2 into sp^3 after chemisorption, indicating the retention of aromaticity of the phenyl ring.. This conclusion is further supported by the preservation of the characteristic vibrational modes [ν(C-C)] of monosubstituted phenyl ring around 1550-1650, 1400-1515, and 1150-1350 cm^{-1} [18, 19] in chemisorbed acetophenone-d_3. More importantly, the nearly unshifted peak at 2275 cm^{-1} assigned to C(sp^3)-D (-CD_3) in Figure 6.7b and the absence of a peak around 2900 cm^{-1} in the spectrum of chemisorbed acetophenone-α-d_3 confirm our assignment of the peak at 2930 cm^{-1} of chemisorbed acetophenone (Figure 6.6b) to the CH_3 stretching mode from the carbonyl methyl group. The absence of vibrational feature for C=O stretching mode (at 1695 cm^{-1}) together with retention of the characteristic vibrational modes [ν(C-C)] of monosubstituted phenyl ring demonstrates that the chemical binding occurs mainly through the external C=O group. Thus, the [2+2]-like cycloaddition between C=O group and Si dimer is the proposed binding mode.

6.4 DFT calculations

In general, there are five possible binding modes for benzaldehyde and acetophenone chemically binded on Si(100), as schematically presented in Figures 6.8 and 6.9, respectively. The direct interaction between phenyl ring and Si dimer is presented in modes II–V. In addition, there is one possibility of the direct participation of the external C=O group via a [2+2]-like cycloaddition pathway (mode I). The DFT studies focus on the geometric optimization and adsorption energy calculation for further understanding of the experimental results.

Calculations were performed using SPARTAN package (Ref. 24) for a benzaldehyde and a acetophenone molecule adsorbed onto a starting cluster of Si_9H_{12}, respectively. This cluster with one exposed Si=Si dimer was successfully used in several previous studies [25–28]. Based on the possible binding modes, five benzaldehyde-bonded (Figure 6.8) and acetophenone-bonded (Figure 6.9) calculation clusters were built to model their corresponding cycloadducts. All DFT studies are single point energy calculation of B3LYP/6-311+G(d) on the fully optimized geometry of B3LYP/6-31G(d). The calculated adsorption energies of binding modes I–V for benzaldehyde and acetophenone are listed in Table 3 and Table 4, respectively. It is unambiguous that the product of [2+2]-like cycloaddition reaction occurring between the external C=O group and Si=Si dimer (mode I) has the largest adsorption energy. Its value is also much higher than that of [4+2]-like cycloadduct (modes IV, V) involving two conjugated C=C bond on phenyl ring and [2+2]-like cycloaddition through a C=C bond on phenyl ring (modes II, III). The calculation result clearly shows that the energetically preferred reaction mechanism for benzaldehyde and acetophenone is the [2+2]-like cycloaddition through

the carbonyl group. This preferable [2+2]-like cycloaddition mechanism for benzaldehyde and acetophenone is similar to benzonitrile on Si(100)-2×1 via the [2+2]-like approach occurring at C≡N group to form a benzoimine-like conjugation skeleton [4]. In both cases, the cycloaddition results in an energetically stable aromatic skeleton on surfaces.

6.5 Discussion

Taguchi et al.[1] found that the C-H stretching feature presents two isolated peaks at 3065 (sp^2 C-H) and 2935 (sp^3 C-H) cm^{-1} in chemisorbed benzene on Si(100) (under a HREELS resolution of fwhm 65 cm^{-1}) due to the rehybridization of carbon atoms of benzene from sp^2 to sp^3. Our HREELS measurements of chemisorbed benzaldehyde and acetophenone (with a resolution of fwhm 55 cm^{-1}) show that all the vibrational modes related to C-H of phenyl ring remain unchanged. This observation, together with the absence of the stretching mode of C=O group, excludes the possible binding modes involving only the carbon atoms of the phenyl ring (modes II, III, IV, V in Figures 6.8 and 6.9). Hence, the vibrational features of chemisorbed benzaldehyde and acetophenone conclusively demonstrate that benzaldehyde and acetophenone selectively bond to Si(100) through the interaction between the carbonyl group and a Si=Si dimer to form Si-C and Si-O linkages via the 1,2-dipolar cycloaddition (mode I in Figures 6.8 and 6.9). This conclusion is consistent with the observation in STM experiment, in which a predominant protrusion appears for benzaldehyde adsorbed on Si(100)-2×1.

Using DFT calculations, it has recently been proposed that the carbonyl group bonded to the surface silicon atoms involves a dative-bonded precursor [8]. The oxygen atom has a couple of lone-pair electrons. Thus, it can possibly act as a donor to provide

electrons to form a dative-bonded precursor with electron-deficient Si dangling bonds, thereby lowering the energy barrier of the surface reaction. This possibly explains the selectivity from the kinetic point of view. On the other hand, the present calculation results reveal that the [2+2]-like cycloaddition through the carbonyl group is thermodynamically favored compared to the [4+2]-like cycloadditions and the [2+2]-like cycloadditions through two conjugated or a C=C bond of the phenyl ring. Thus, benzaldehyde and acetophenone selectively bonded to Si(100) through the interaction between the carbonyl group and a Si=Si dimer via the 1,2-dipolar cycloaddition is thermodynamically and kinetically preferred.

6.6 Conclusions

Our experimental results together with DFT calculations have shown that both benzaldehyde and acetophenone covalently bind to Si(100)-2×1 through the [2+2]-like cycloaddition reaction between the external C=O group and Si=Si dimer, leaving its phenyl ring skeleton intact. The phenyl ring skeleton may possibly be employed as precursors for further chemical modification and functionalization of silicon surfaces.

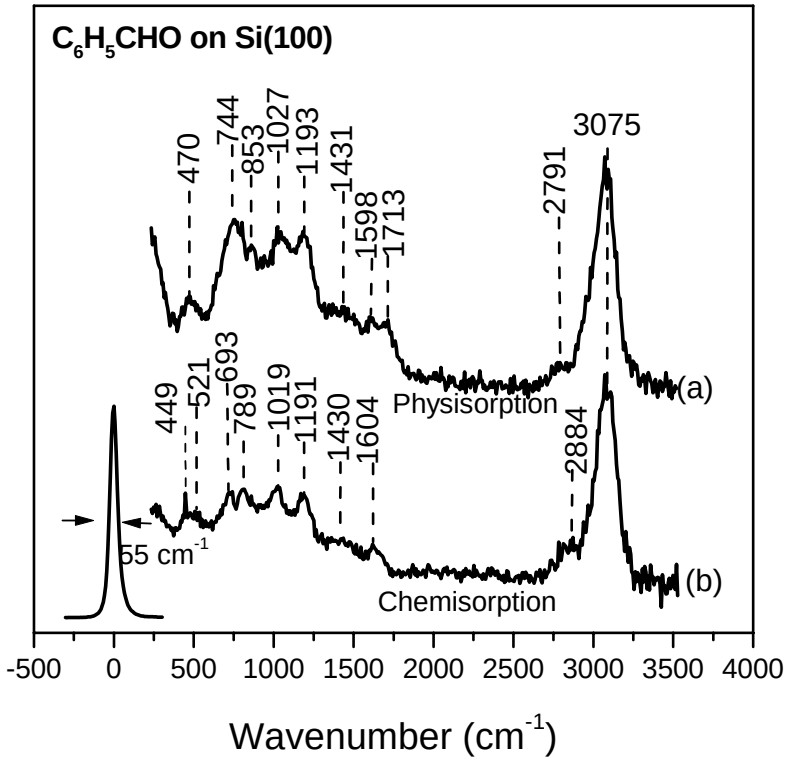

Figure 6.1 HREELS spectra of the physisorbed and the saturated chemisorbed benzaldehyde on Si(100)-2×1.

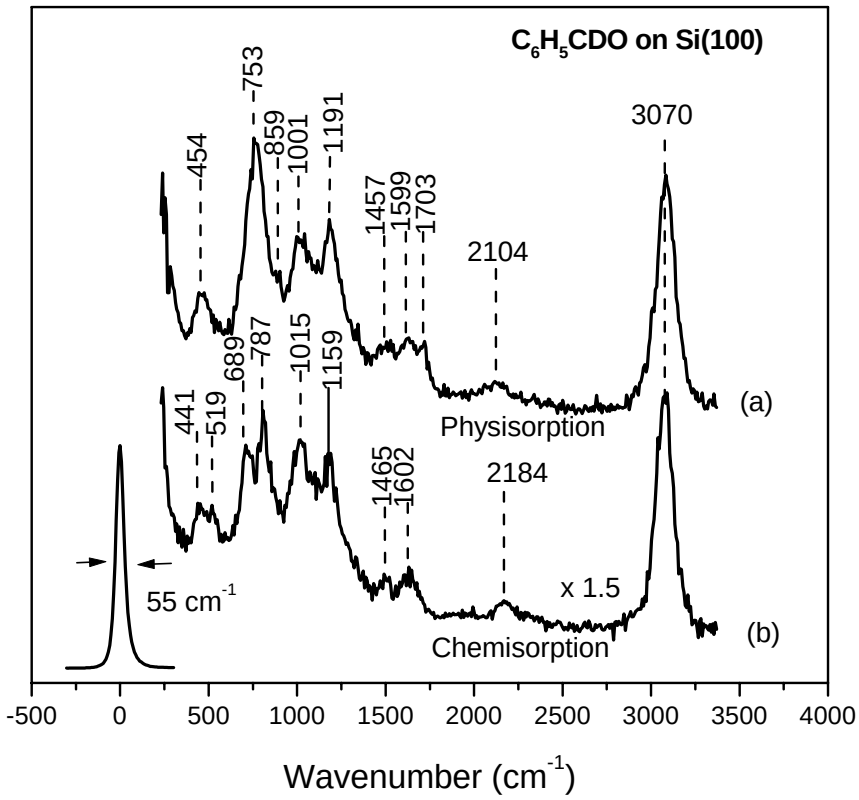

Figure 6.2 HREELS spectra of physisorbed and saturated chemisorbed benzaldehyde-α-d_1 on Si(100)-2×1.

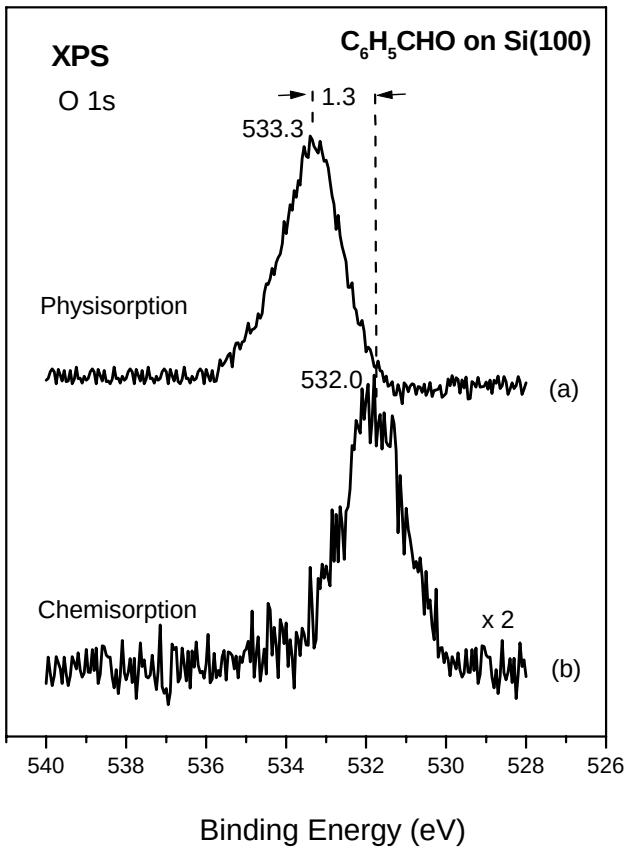

Figure 6.3 O 1s XPS spectra for physisorbed and chemisorbed benzaldehyde on Si(100)-2×1

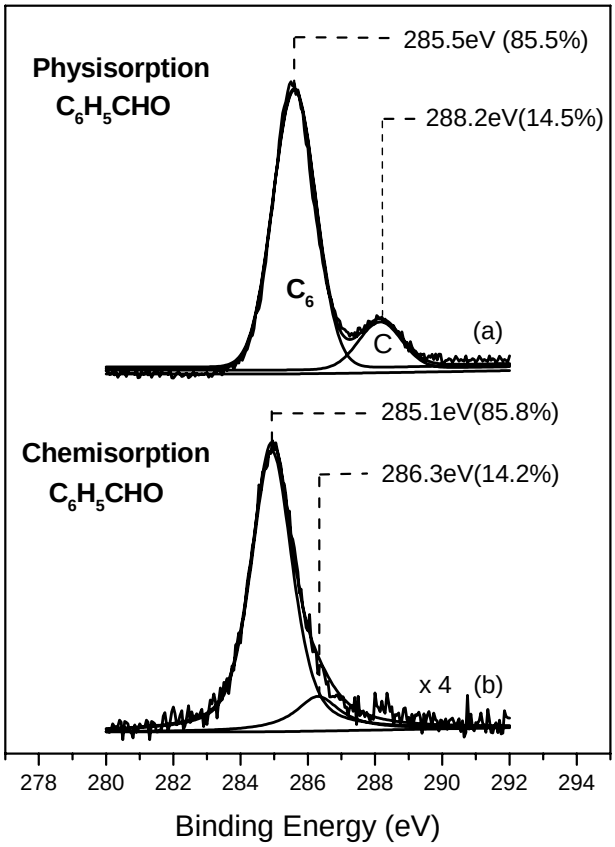

Figure 6.4 Fitted C 1s XPS spectra for physisorbed and saturated chemisorbed benzaldehyde on Si(100)-2×1.

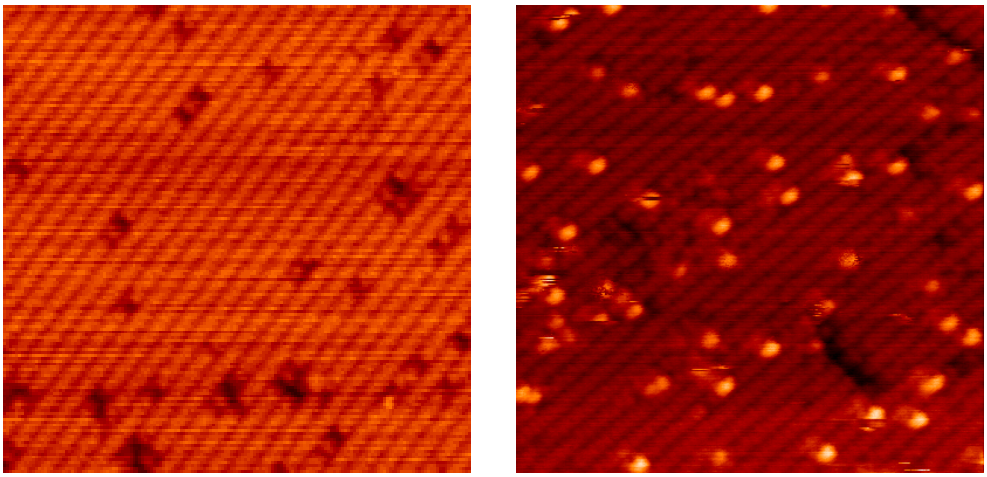

(a) (b)

Figure 6.5 STM constant-current-topograph (CCT) (20 × 20 nm, V_s=-2.0.0V, I_T=0.15nA) images of clean Si(100)-2×1 (a) and Si(100)-2×1 after exposure to 0.01 L of benzaldehyde at 300 K (b).

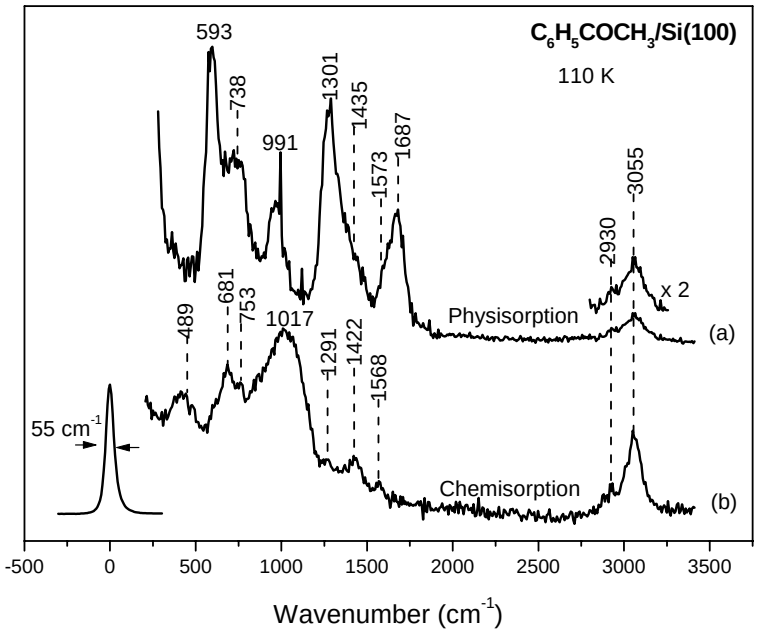

Figure 6.6 HREELS spectra of the physisorbed and saturated chemisorption acetophenone on Si(100)-2×1.

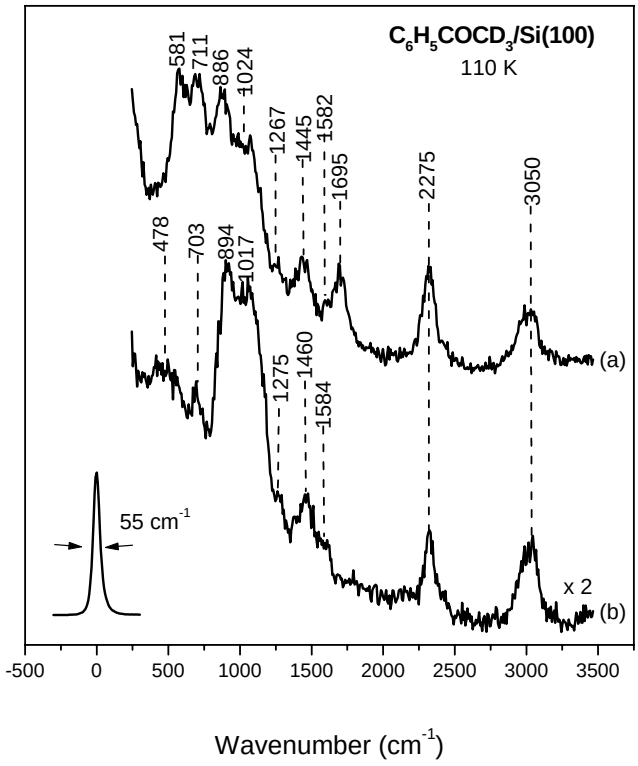

Figure 6.7 HREELS spectra of physisorbed and saturated chemisorbed acetophenone-α-d_3 on Si(100)-2×1.

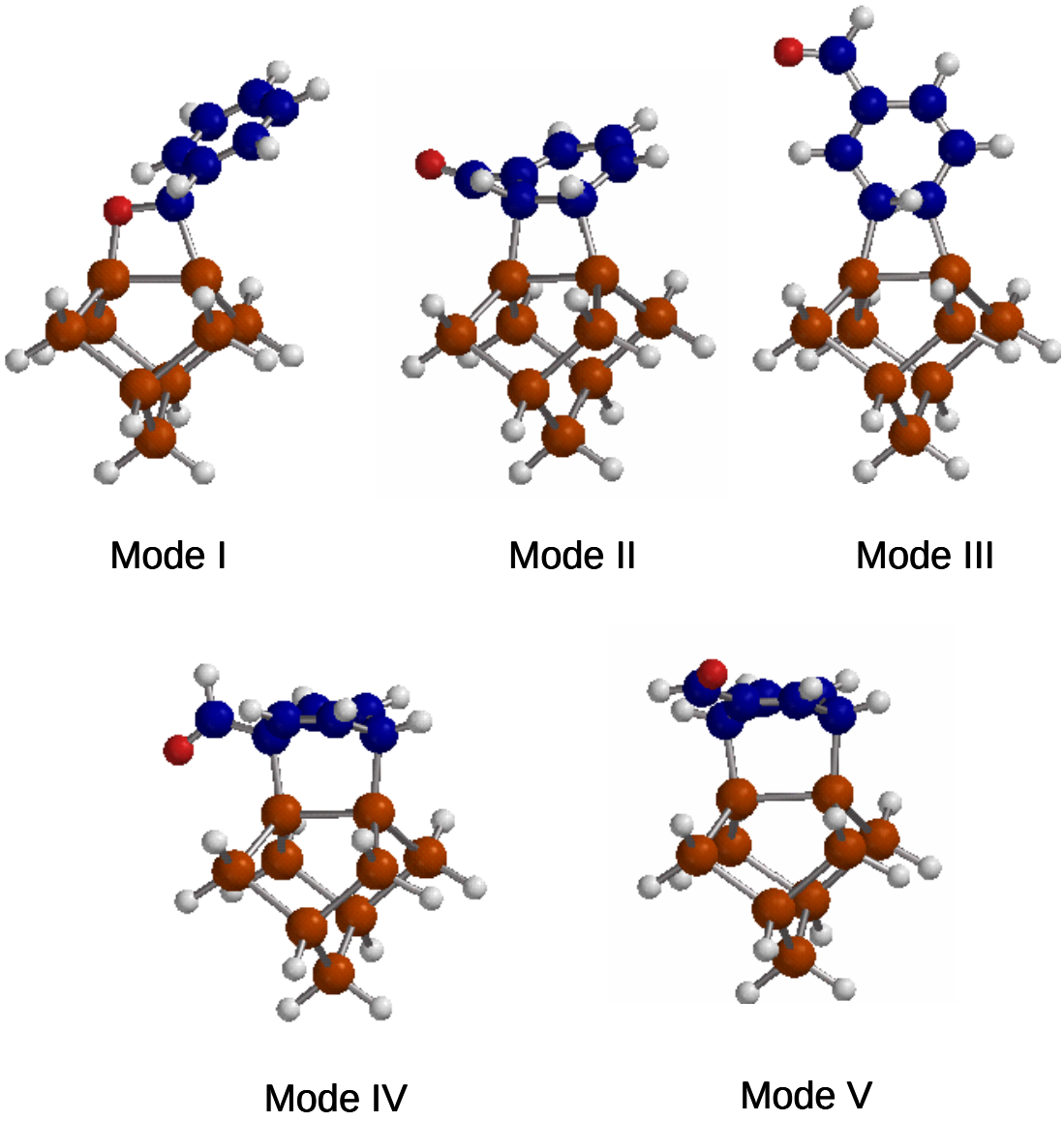

Figure 6.8 Optimized benzaldehyde/Si_9H_{12} clusters corresponding to the five possible attachment modes through [2+2]-like and [4+2]-like addition reactions.

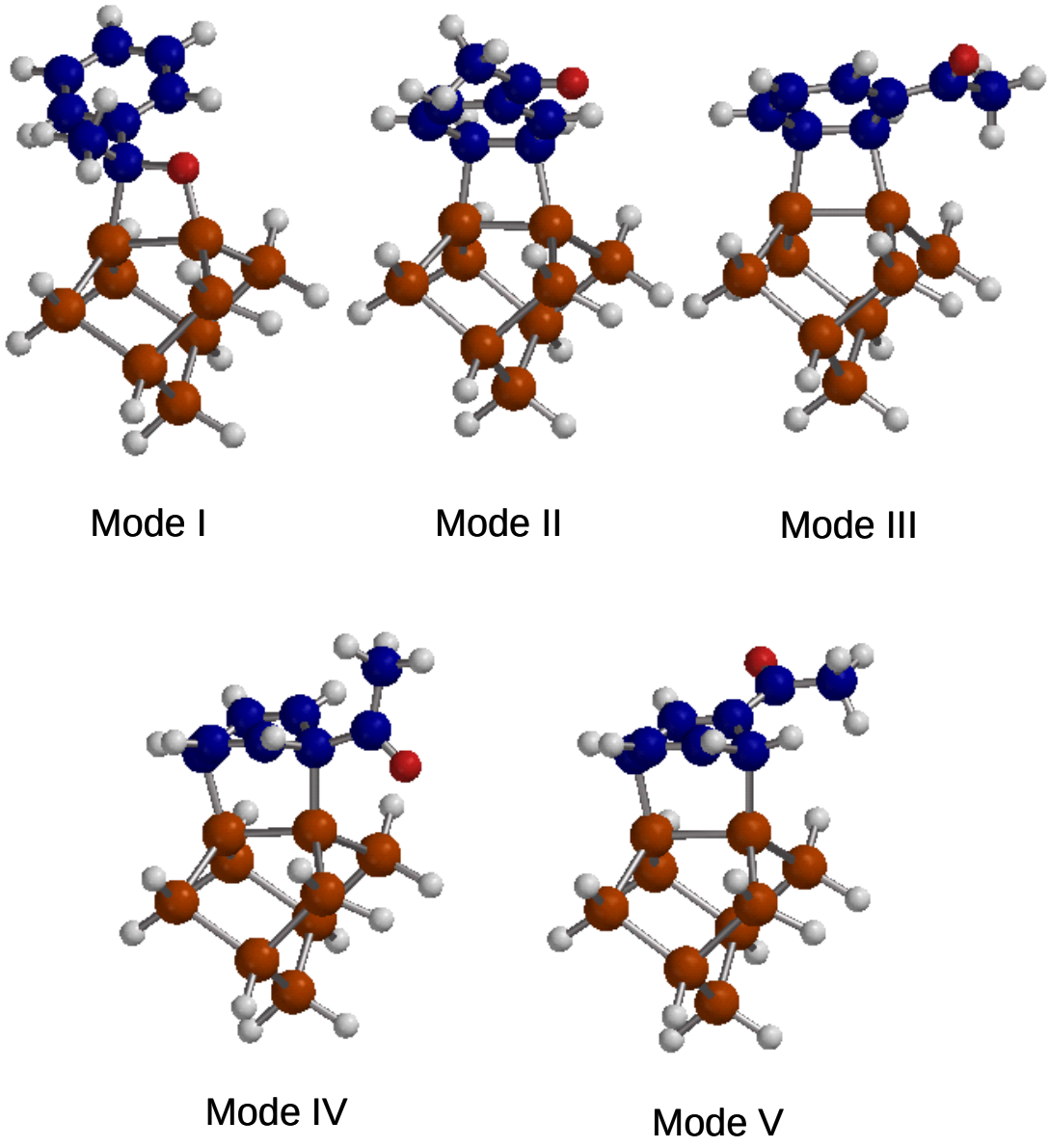

Figure 6.9 Optimized acetophenone/Si_9H_{12} clusters corresponding to the five possible attachment modes through [2+2]-like and [4+2]-like addition reactions.

Table 6.1 Vibrational modes assignment for physisorbed and chemisorbed benzaldehyde on Si(100)-2×1. IR data (Ref. 15) for liquid benzaldehyde is included for comparison. All vibrational frequencies are given in cm^{-1}. Phys.: Physisorbed molecules; Chem.; Chemisorbed molecules.

Description	IR liquid	Phys.	Chem.	Isotope	Phys.	Chem.
ν C-H	3084, 3063, 3036, 3026	3075	3075	3082, 3061, 3030, 3006	3070	3070
ν CH(D)	2806	2791	2884	2110	2104	2184
ν C=O	1703	1713		1695	1703	
ν C-C	1596	1598	1604	1587	1599	1602
ν C-C	1456	1431	1430	1456	1457	1465
δ CH(D)	1387			1044		
ν C-C	1203	1193	1191	1214	1191	1159
β C-H	1164, 1158, 1069, 1021 1000	1027	1019	1167, 1162, 1074, 1022 1002	1001	1015
γ C-H	978					
ϕ C-C	827	853	789	788	859	787
	744	744			753	
ν Si-O			693			689
ν Si-C			521			519
ϕ C-C	449, 226	470	449	445	454	441

Table 6.2 Vibrational modes assignment for physisorbed and chemisorbed acetophenone on Si(100)-2×1. IR data (Ref. 21) for liquid acetophenone is included for comparison. All vibrational frequencies are given in cm^{-1}. Phys.: Physisorbed molecules; Chem.; Chemisorbed molecules.

Description	IR liquid	Phys.	Chem.	Isotope	Phys.	Chem.
ν C-H	3088, 3067, 3061, 3030	3055	3055	3086, 3065, 3060, 3031	3050	3050
ν $CH(D)_3$	2925	2930	2930	2255	2275	2275
ν C=O	1685	1687		1683	1695	
ν C-C	1582	1573	1568	1581	1582	1584
ν C-C	1450	1435	1422	1450	1445	1460
δ $CH(D)_3$	1360			983		
ν C-C	1312	1301	1291	1313	1267	1275
β C-H	1181, 1161, 1078,			1181, 1160, 1074,		
ρ $CH(D)_3$	1021			874	886	893
Ring	1000	991	1017	1002	1009	1017
γ C-H	955					
ϕ C-C	730	738	753	728	711	
ν Si-O			681			694
β C=O	590	593		584	581	
ν Si-C			489			493
ϕ C-C	547			548		
γ C_{Ar}-C-C	368			350		
ϕ C-C	226			226		

Table 6.3. Adsorption energies of the local minima in the benzaldehyde / Si_9H_{12} Model system from pBP/DN.

Binding model	I	II	III	IV	V
Reaction model	[2+2]	[2+2]	[2+2]	[4+2]	[4+2]
Adsorption energy [a]	37.2	-5.59	-0.92	12.8	19.3

[a] Adsorption energy: $\Delta E = [E(Si_9H_{12}) + E(C_7H_6O)] - E(C_7H_6O/Si_9H_{12})$. All energies are in kcal mol^{-1}.

Table 6.4. Adsorption energies of the local minima in the acetophenone / Si_9H_{12} Model system from pBP/DN.

Binding model	I	II	III	IV	V
Reaction model	[2+2]	[2+2]	[2+2]	[4+2]	[4+2]
Adsorption energy [a]	29.6	-11.1	-2.41	5.55	18.54

[a] Adsorption energy: $\Delta E = [E(Si_9H_{12}) + E(C_8H_8O)] - E(C_8H_8O/Si_9H_{12})$. All energies are in kcal mol^{-1}.

Reference:

1. Y. Taguchi, M. Fujisawa, T. Takaoka, Y. Okada, M. Nishijima, J. Chem. Phys. **95**, 6870 (1991).
2. G.P. Lopinski, T.M. Fortier, D.J. Moffatt, R.A. Wolkow, J. Vac. Sci. Technol. A **16**, 1037(1998).
3. G.P. Lopinski, D.J. Moffatt, R.A. Wolkow, Chem. Phys. Lett. **282**, 305 (1998).
4. F. Tao, Z. H. Wang, G. Q. Xu. J. Phys. Chem. B **106**, 3557(2002).
5. J.L. Armstrong, E.D. Pylant, J.M. White, J. Vac. Sci.Technol. A **16**, 123 (1998).
6. J.L. Armstrong, J.M. White, M. Langell, J. Vac. Sci. Technol. A **15**, 1146 (1997).
7. E. D. Pylant, M. J. Hubbard, and J. M. White, J. Phys. Chem. **100**, 15890 (1996).
8. J. A. Barriocanal, D. J. Doren, J. Am. Chem. Soc. **123**, 7340 (2001).
9. L. Fang, J. M. Liu, S. Coulter, X. P. Cao, M. P. Schwartz, C. Hacker, R. J. Hamers, Surf. Sci. **514**, 362 (2002).
10. G.T. Wang, C. Mui, C.B. Musgrave, S.F. Bent, J. Am. Chem. Soc. **124**, 8990 (2002).
11. C. A. Hacker, R. J. Hamers, J. Phys. Chem. B **107**, 7689 (2003).
12. C. Hamai, A. Takagi, M. Taniguchi, T. Matsumoto, T. Kawai. Angew. Chem. Int. ed. **43**, 1349 (2004).
13. S.K. Coulter, J.S. Hovis, M.D. Ellison, R.J. Hamers, J. Vac. Sci. Technol. A **18,** 1965 (2000).
14. B. Borovsky, M. Krueger, E. Ganz, J. Vac. Sci. Technol. B **17**, 7 (1999).
15. J. H. S. Green, D. J. Harrison, Spectrochimica Acta, **32**, 1265 (1976).
16. Y. J. Chabal, K. Raghavachari, Phys. Rev. Lett. **53**, 282 (1984).
17. X. Lu, M. C. Lin, Int. Rev. Phys. Chem. **21**, 137 (2002).

18. L. V. Daimay, B. C. Norman, G. F. William, and G. G. Jeanette, The Handbook of Infrared and Raman Characteristic Frequencies of Organic Molecules, (Academic, Boston, 1991).
19. G. Varsanyi and S. Szoke, Vibrational Spectra of Benzene Derivates (Academic, New York & London, 1969).
20. F. Tao, M. H. Qiao, H. L. Zhen, L. Yang, Y. J. Dai, H. G. Huang, G. Q. Xu, Phys. Rev. B.**67**, 115334-1 (2003).
21. J. H. S. Green, D. J. Harrison, Spectrochimica Acta, **33**, 583 (1977).
22. Y. Cao, Z. H. Wang, J. F. Deng, G. Q. Xu, Angew. Chem. Int. Edt.**39**, 2740 (2000).
23. J. Y. Huang, H. G. Huang, K. Y. Lin, Q. P. Liu, Y. M. Sun, G. Q. Xu, Surf. Sci. **549**, 255 (2004).
24. M. J. Frisch, G. W. Trucks, H. B. Schlegel, P. M. W. Gill, B. G. Johnson, M. A. Robb, J. R. Cheeseman, T. Keith, G. A. Petersson, J. A. Montgomery, K. Raghavachari, M. A. Al-Laham, V. G. Zakrzewski, J. V. Ortiz, J. B. Foresman, J. Cioslowski, B. B. Stefanov, A. Nanayakkara, M. Challacombe, C. Y. Peng, P. Y. Ayala, W. Chen, M. W. Wong, J. L. Andres, E. S. Replogle, R. Gomperts, R. L. Martin, D. J. Fox, J. S. Binkley, D. J. Defrees, J. Baker, J. P. Stewart, M. Head-Gordon, C. Gonzalez, and J. A. Pople, GAUSSIAN 94, Rev. C. W (Gaussian, Inc. Pittsburgh, PA, 1995).
25. T. Kato, S. Y. Kang, X. Xu, and T. Yamabe, J. Phys. Chem. B **105**, 10340 (2001).
26. X. Xu, S. Y. Kang, and T. Yamabe, Bull. Chem. Soc. Jpn. **74**, 817 (2001).
27. P. L. Silvestrelli, F. Ancilotto, and F. Toigo, Phys. Rev. B **62**, 1596 (2000).
28. H. A. Hofer, A. J. Fisher, G. P. Lopinski, and R. A. Wolkow, Phys.Rev. B **63**, 085314 (2001).